

# ornl

ORNL/TM-10386  
ENDF-343

**OAK RIDGE  
NATIONAL  
LABORATORY**

**MARTIN MARIETTA**

## **Evaluation of the Neutron Cross Sections for Pu-240**

L. W. Weston  
E. D. Arthur

OPERATED BY  
MARTIN MARIETTA ENERGY SYSTEMS, INC.  
FOR THE UNITED STATES  
DEPARTMENT OF ENERGY

Printed in the United States of America. Available from  
National Technical Information Service  
U.S. Department of Commerce  
5285 Port Royal Road, Springfield, Virginia 22161  
NTIS price codes—Printed Copy: A03; Microfiche A01

This report was prepared as an account of work sponsored by an agency of the United States Government. Neither the United States Government nor any agency thereof, nor any of their employees, makes any warranty, express or implied, or assumes any legal liability or responsibility for the accuracy, completeness, or usefulness of any information, apparatus, product, or process disclosed, or represents that its use would not infringe privately owned rights. Reference herein to any specific commercial product, process, or service by trade name, trademark, manufacturer, or otherwise, does not necessarily constitute or imply its endorsement, recommendation, or favoring by the United States Government or any agency thereof. The views and opinions of authors expressed herein do not necessarily state or reflect those of the United States Government or any agency thereof.

Engineering Physics and Mathematics Division

EVALUATION OF THE NEUTRON CROSS SECTIONS FOR PU-240

L. W. Weston and E. D. Arthur\*

Manuscript Completed: March 1987  
Date Published: April 1987

Research sponsored by  
U.S. DOE Office of  
Basic Energy Sciences

\*Los Alamos National Laboratory, Los Alamos, New Mexico 87545

Prepared by the  
OAK RIDGE NATIONAL LABORATORY  
Oak Ridge, Tennessee 37831  
operated by  
Martin Marietta Energy Systems, Inc.  
Under Contract No. DE-AC05-84OR21400  
for the  
U.S. Department of Energy



## TABLE OF CONTENTS

Abstract . . . . .	1
1. Thermal Neutron Energy Region . . . . .	1
2. Resolved Resonance Region . . . . .	3
3. Unresolved Resonance Region . . . . .	5
4. Smooth Cross Section . . . . .	7
5. Angular and Energy Distributions of Neutrons . . . . .	18
5.1 Elastic Scattering . . . . .	18
5.2 Inelastic Scattering . . . . .	18
5.3 Neutron Energy Distributions . . . . .	18
6. Other Files . . . . .	18
7. Conclusions . . . . .	19
Acknowledgments . . . . .	20



# EVALUATION OF THE NEUTRON CROSS SECTIONS FOR PU-240

## ABSTRACT

The present evaluation is proposed to supersede the ENDF/B-V, Revision 2 file for  $^{240}\text{Pu}$  by L. W. Weston *et al.*, dated September, 1978.<sup>1-3</sup> In this work, resonance parameters, cross sections, energy distributions, and angular distributions have been modified. These changes are outlined in detail and appropriate references included.

### 1. THERMAL NEUTRON ENERGY REGION

The thermal neutron cross sections are defined by the resolved resonance parameters and therefore may be calculated at any desired temperature. Table 1 gives the calculated 2200 m/s cross sections at room temperature for ENDF/B-V and the present evaluation. The cross sections were calculated using the code NPTXS by R. Q. Wright. The differences are due to changes in the parameters of the 1.056-eV resonance and the uncertainties are determined by the uncertainties in these parameters.

Table 1. Calculated 2200 m/s cross sections

	Capture (barns)	Scattering (barns)	Fission (barns)	Total (barns)
ENDF/B-V	$289.8 \pm 2.9$	1.55	$0.057 \pm 0.019$	291.4
Present evaluation	$287.6 \pm 2.9$	0.96	$0.064 \pm 0.019$	288.6

The thermal neutron energy region for  $^{240}\text{Pu}$  is dominated by the resonance at 1.056-eV, which contributes more than 98% of the cross section at 2200 m/s. Traditionally, discrepancies in the measured parameters of the 1.056-eV resonance<sup>4,5</sup> make the parameters difficult to evaluate to the needed accuracy. Uniform samples, which must be very thin because of the size of the resonance, are difficult to fabricate. Also, the resolution function and the Doppler width of the resonance in this transition region

of neutron energy must be known and understood. Table 2 gives the ENDF/B-IV, ENDF/B-V, and present evaluated values for the resonance parameters of the 1.056-eV resonance; the most accurate reported integral determination of the 2200 m/s absorption cross section;<sup>6</sup> and two recent measurements of the resonance parameters.<sup>7,8</sup>

Table 2. Parameters of the 1.056-eV resonance

Source	Neutron width (meV)	Radiation width (meV)	Product (meV) <sup>2</sup>	2200 m/s capture cross section (barns)
ENDF/B-IV	2.44	29.9	73.0	277
ENDF/B-V	2.28 ± 0.15	33.3 ± 2.0	75.9 ± 0.7	289.8 ± 2.9
Lounsbury <i>et al.</i> <sup>6</sup>			75.8 ± 0.4 <sup>a</sup>	289.5 ± 1.4
Liou & Chrien <sup>7</sup>	2.32 ± 0.06	32.4 ± 0.6	75.2 ± 2.4	288.3 ± 9.0 <sup>a</sup>
Spencer <i>et al.</i> <sup>8</sup>	2.45 ± 0.02	30.3 ± 0.3	74.2 ± 0.6	284.8 ± 2.0 <sup>a</sup>
Present evaluation	2.45 ± 0.02	30.6 ± 0.6	75.0 ± 0.6	287.6 ± 2.9 <sup>a</sup>

<sup>a</sup>Calculated assuming 4.0 barns contribution from all other resonances.

An integral measurement of the 2200 m/s absorption cross section was made by Lounsbury *et al.*<sup>6</sup> in a thermal column. This measurement can be interpreted as the product of the neutron and radiation widths. Liou and Chrien<sup>7</sup> measured the transmission and capture cross sections of metal and oxide samples at room, liquid nitrogen, and liquid helium temperatures. Spencer *et al.*<sup>8</sup> used multiple sample thicknesses at room temperature to carefully measure the transmission.

The ENDF/B-IV evaluation reflects earlier measurements of the resonance parameters of the 1-eV resonance and the 2200 m/s cross sections. For ENDF/B-V, a higher radiation width was chosen in an attempt to obtain better agreement with reactor burn-up calculations.<sup>4</sup> Two recent, accurate differential measurements, which are now available, do not justify this choice. Instead, the present values are evaluated from the recent measurements. These measurements are slightly discrepant, however, no known reason has been found to discount either of the measurements.

## 2. RESOLVED RESONANCE REGION

The resolved resonance region extends from  $10^{-5}$  eV to 5.7 keV. From 20 to 3,900 eV the neutron widths of the resonances are essentially unchanged from ENDF/B-V where they were derived from weighted averages of the results reported by Weigmann,<sup>9</sup> Ashgar,<sup>10</sup> and Hockenbury.<sup>11</sup> From 3,900 to 5,700 eV, where the present evaluation has been expanded, the neutron widths are essentially those determined by Kolar and Böckhoff.<sup>12</sup> The neutron widths of resonances with very large subthreshold fission widths were reevaluated in some cases.

From 2,680 to 5,700 eV, a smooth cross section was added to the total and capture cross sections in File 3 to account for the missed resonances. The magnitude of the missed resonances was derived by plotting the sum of the neutron widths versus neutron energy as shown in Fig. 1. The missed levels, the area between the two curves in Fig. 1, were assumed to be narrow so that  $\Gamma_n \ll \Gamma_\gamma$  and:

$$\langle \sigma \rangle = 2\pi^2 \chi^2 E^{1/2} [\Gamma_n^0/D - S]$$

where  $\langle \sigma \rangle$  is the correction to the cross section,  $\Gamma_n^0/D$  is the s-wave strength function ( $1.05 \times 10^{-4}$ ) at low neutron energies where no levels are missed and  $S$  is the effective, measured strength function ( $0.73 \times 10^{-4}$ ) at higher neutron energies.

The fission resonance areas of most of the resonances have been reported by Weston and Todd<sup>13</sup> since the ENDF/B-V evaluation. The fission widths for the present evaluation are essentially the weighted averages of these derived widths and those of Auchampaugh and Weston,<sup>14</sup> and Migneco and Theobald.<sup>15</sup> Figure 2, taken from Ref. 13, shows the character of the subthreshold fission cross section. The fission cross section exhibits the intermediate structure due to levels in the second well of the double-humped fission barrier.

ORNL-DWG 86-15448

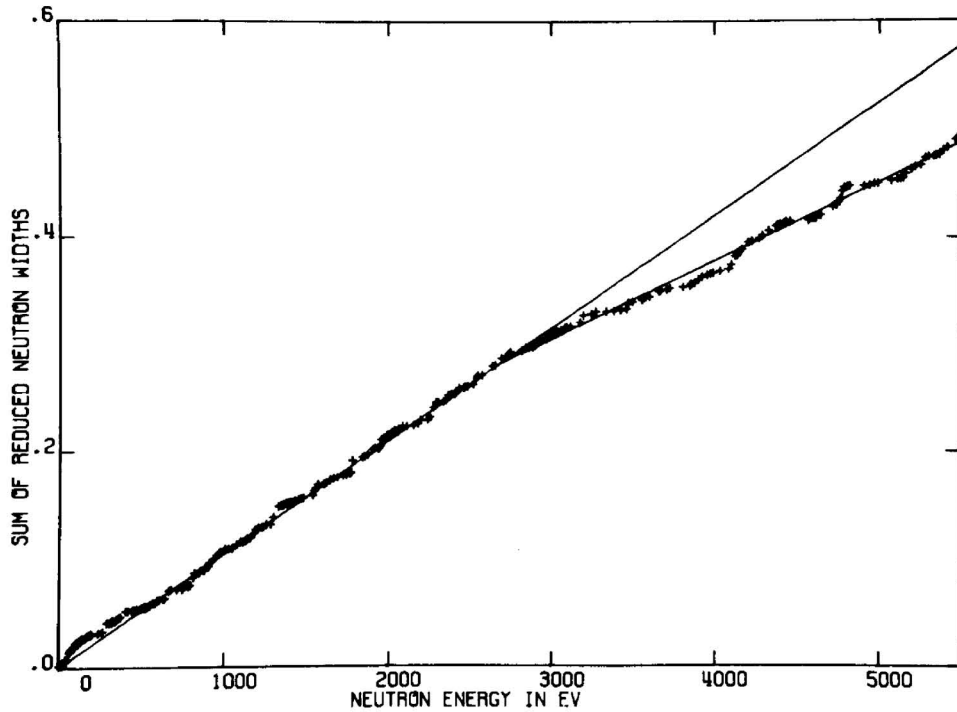


Figure 1. Sum of the reduced resonance neutron widths versus neutron energy in the resolved resonance region. The area between the diverging lines indicates levels missed due to instrumental resolution.

ORNL-DWG 83-19644

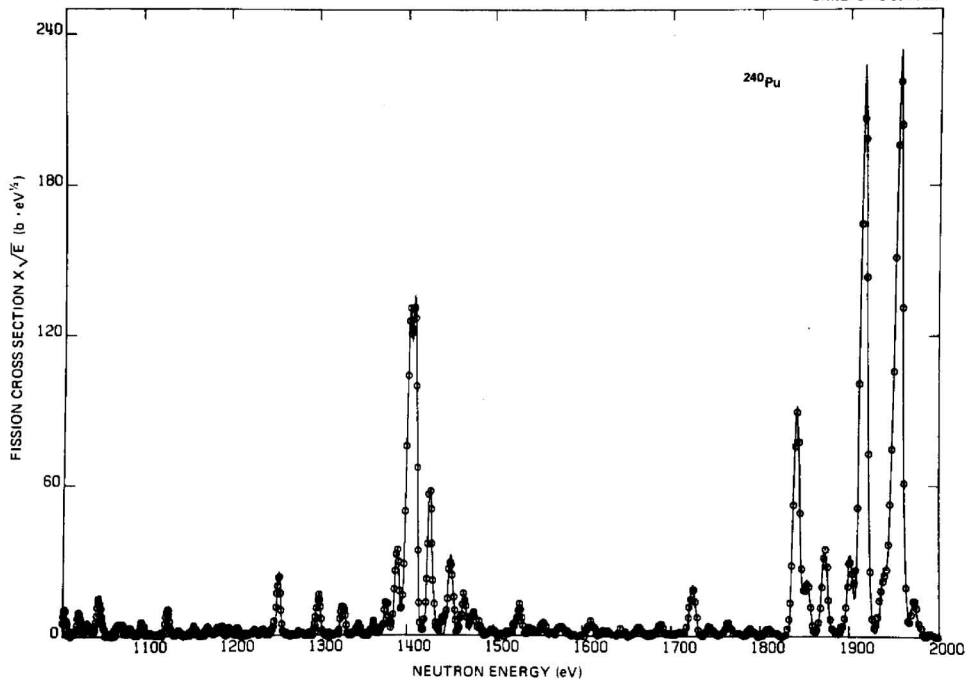


Figure 2. Example of the subthreshold fission resonances. The clumps of resonances are due to resonances in the second well of the double humped fission barrier.

Uncertainties in the resolved resonance region are dominated by the 1-eV and first few higher resonances. The uncertainties of the first few resonances above 1 eV are unchanged from Version V.

### 3. UNRESOLVED RESONANCE REGION

The unresolved resonance region for this evaluation extends from 5.7 to 40 keV where the first inelastic scattering level is located. The unresolved resonance region for ENDF/B-V extends from 3.9 to 40 keV.

Since the ENDF/B-V evaluation, the average total cross sections have been measured by Gwin *et al.*,<sup>16</sup> Poenitz *et al.*,<sup>17</sup> and Käppeler *et al.*<sup>18</sup> Three measurements of the capture cross sections have been reported; those by Weston and Todd,<sup>19</sup> Wisshak and Käppeler,<sup>20</sup> and Hockenbury *et al.*<sup>11</sup> These measurements were fit simultaneously for average resonance parameters using the code, FITACS, provided by F. H. Fröhner.<sup>21</sup> The total cross-section measurements by Käppeler *et al.*<sup>18</sup> were given zero weight because of discrepancies with other measurements and the fact that the Käppeler data were difficult to fit with reasonable average resonance parameters. Figures 3 and 4 illustrate the fit to the total and capture cross sections. The derived average resonance parameters are:

$$\begin{aligned}
 S_0 &= 1.2 \times 10^{-4} \\
 S_1 &= 2.3 \times 10^{-4} \\
 \Gamma_\gamma &= 31 \text{ meV (from resonance region)} \\
 D &= 13.1 \text{ eV}
 \end{aligned}$$

The fit was sensitive to  $S_0$ ,  $S_1$ , the ratio  $\Gamma_\gamma/D$ , and the average fission cross section. The ratio,  $\Gamma_\gamma/D$ , was assumed to be the same for s-wave and p-wave neutrons. These parameters are consistent with those evaluated by Mughabghab<sup>22</sup> except for  $S_0$  which he quoted as  $0.93 \pm 0.08$ . The s-wave strength function of  $1.2 \times 10^{-4}$  was determined predominately by the transmission measurements of Gwin.<sup>16</sup> There could be a variation in  $S_0$  of this difference since the lower value was determined from the resolved resonance region at lower neutron energies.

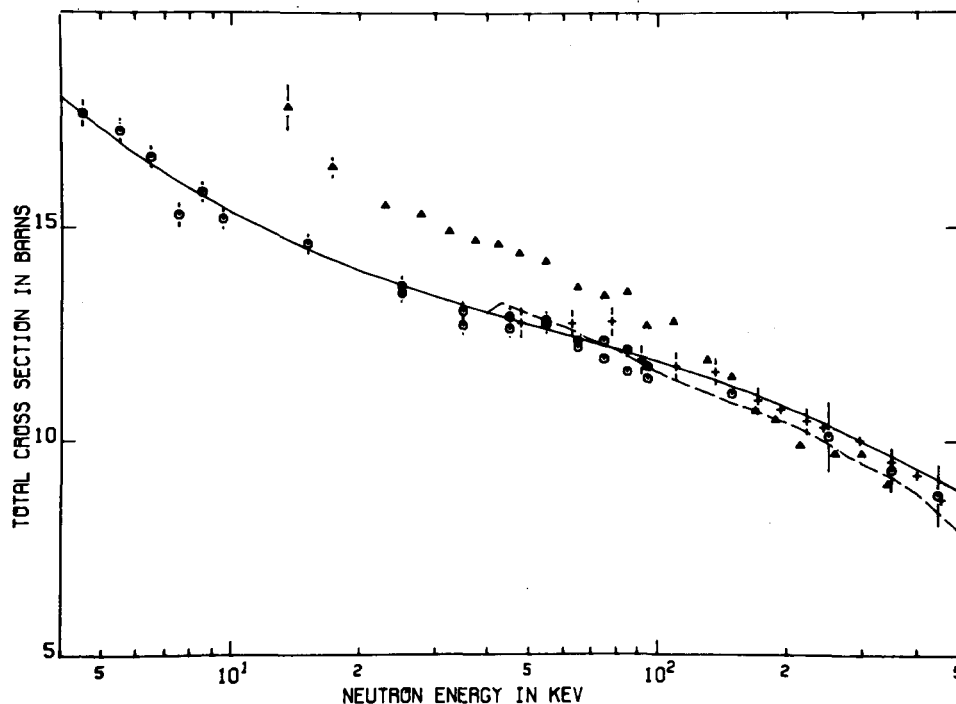


Figure 3. Fit to the total cross section (solid line). The circles are the data of Gwin.<sup>16</sup> The pluses are the data of Poenitz *et al.*<sup>17</sup> and the triangles are the data of Käppeler *et al.*<sup>18</sup> The dashed line is the ENDF/B-V evaluation.

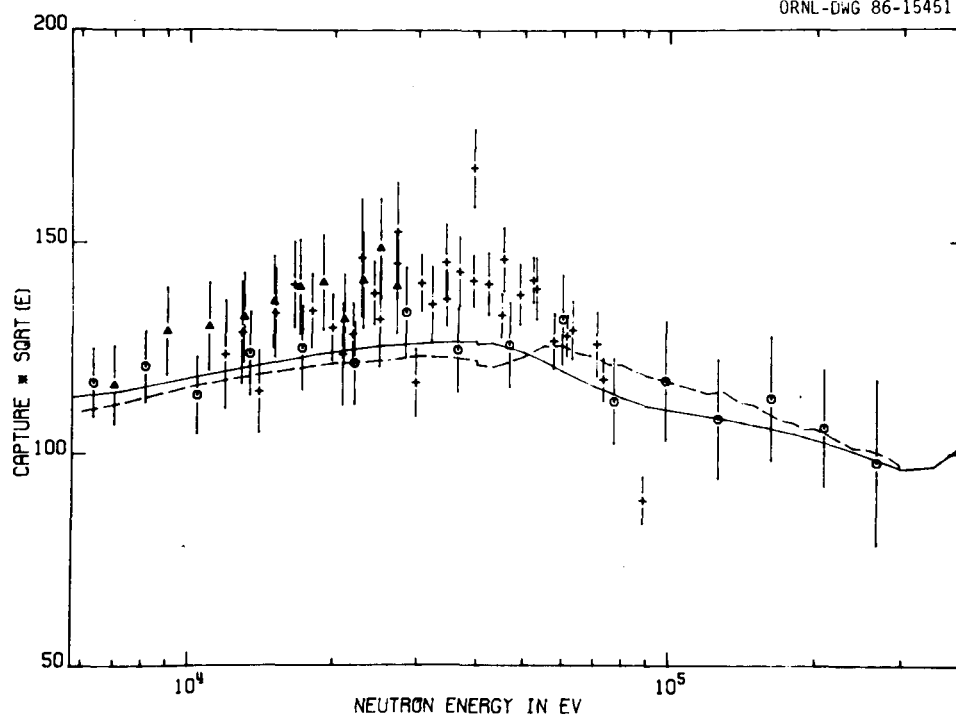


Figure 4. Fit to the capture cross sections of  $^{240}\text{Pu}$  (solid line). The circles are the data of Weston and Todd<sup>19</sup> and the pluses and the triangles are the data of Wisshak and Käppeler.<sup>20</sup> The dashed line is the ENDF/B-V evaluation. The cusp at 43 keV is due to the first inelastic scattering level.

Two recent measurements of the average subthreshold fission cross section in this neutron energy region by Weston and Todd<sup>13</sup> and by Budtz-Jørgensen and Knitter,<sup>23</sup> which are in excellent agreement, were used to evaluate the average fission cross section. These averaged data are shown in Fig. 5. Both data sets show much more structure in this energy region, however, a fit was attempted only to the overall shape and correct integral. Two recent measurements of the ratio of this cross section to that of  $^{235}\text{U}$  by Behrens *et al.*<sup>24</sup> and Wisshak and Käppeler<sup>25</sup> were not directly used in this neutron energy region because of difficulty in interpretation.

Since the shape of this cross section was incompatible with the models used in the FITACS code,<sup>21</sup> the fitted capture and scattering cross sections were modified to reflect the evaluation of the average fission cross section. The code, URES, by E. Pennington<sup>26</sup> was used to make this modification. The strength functions and  $\Gamma_\gamma/D$  from the FITACS fit were used with the fission widths derived with the URES fit.

The capture cross-section evaluation is in good agreement with the measurements of Weston and Todd<sup>19</sup> but not as good with those of Wisshak and Kappelar<sup>20</sup> and Hockenbury *et al.*<sup>11</sup> The total cross section and average resonance parameters from the resonance region had a strong influence on the present evaluation of the capture cross section.

#### 4. SMOOTH CROSS SECTIONS

From 100 to 300 keV the capture cross section is extrapolated from the present fit to the value in ENDF/B-V. Above 300 keV the capture cross section is unchanged from ENDF/B-V in this neutron energy region. Figure 6 compares the Version V and present evaluated capture cross sections above 40 keV with the calculated values of Lagrange and Jary.<sup>27</sup>

The fission cross section from 40 to 100 keV is based on the measurements of Weston and Todd<sup>13</sup> and Budtz-Jørgensen and Knitter<sup>23</sup> (see Fig. 5). From 100 keV to 1 MeV, no changes were made in the evaluation for Version V of the fission ratio to  $^{235}\text{U}$ , which was based primarily on the

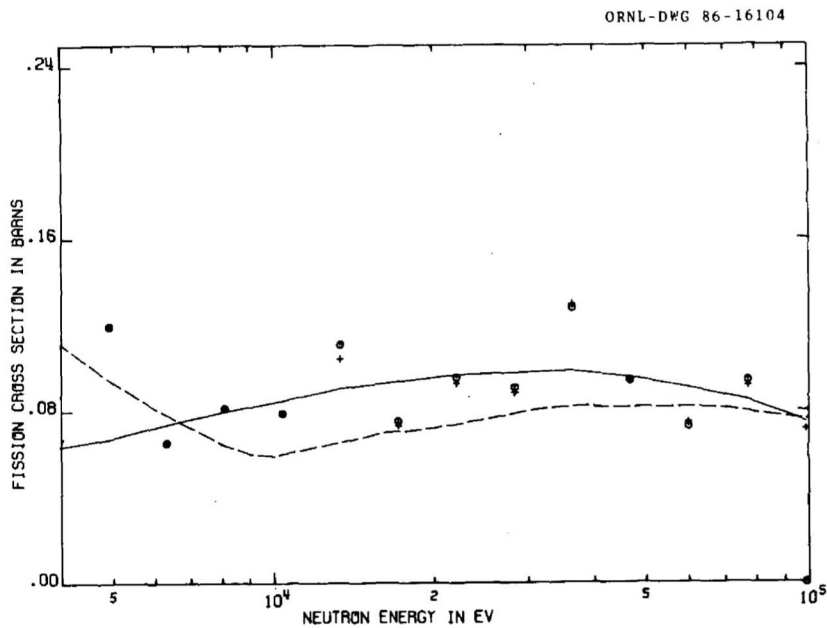


Figure 5. The averaged subthreshold fission cross section for  $^{240}\text{Pu}$ . The circles are the data of Weston and Todd<sup>13</sup> and the pluses the data of Budtz-Jørgensen and Knitter.<sup>23</sup> The solid line is the present evaluation and the dashed line is ENDF/B-V.

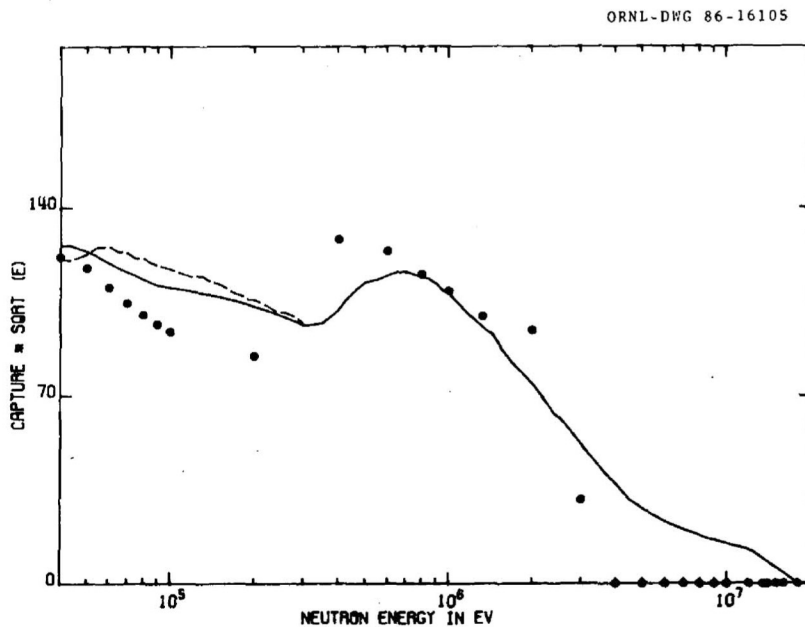


Figure 6. The present evaluation (line) of the capture cross section above 40 keV and the ENDF/B-V evaluation (dashed line). The points are from the model calculation of Lagrange and Jary.<sup>27</sup>

data of Behrens *et al.*<sup>28</sup> Version V is in agreement with the new measurements of Weston and Todd<sup>29</sup> and the ratio measurements of Cierjacks *et al.*,<sup>30</sup> shown in Fig. 7. Figure 8 shows the data of Meadows,<sup>31</sup> Budtz-Jørgensen and Knitter,<sup>23</sup> and the Version V evaluation in the same neutron energy region. If the data of Meadows<sup>31</sup> and Budtz-Jørgensen and Knitter<sup>23</sup> are shifted to lower neutron energies by about 4%, the evaluation is within the uncertainties of most of the measured values. Since the neutron energy scale can usually be determined more accurately for a LINAC measurement, the neutron energy scale of Behrens *et al.*<sup>28</sup> was retained.

Above 1 MeV there are a number of measurements of the ratio of the  $^{240}\text{Pu}$  fission cross section to that of  $^{235}\text{U}$ . Figures 9 and 10 show these data and the ENDF/B-V and the present evaluation. Figure 11 shows the fission cross-section measurement of Kari and Cierjacks<sup>32</sup> and the present evaluation in this neutron energy range. The shape of the Kari fission cross-section measurement<sup>32</sup> was given appreciable weight relative to the fission ratio measurements by Weston and Todd<sup>29</sup> and Behrens *et al.*,<sup>28</sup> because the LINAC measurements had low neutron intensity at these high neutron energies. In this neutron energy range, fission must be separated into first, second, and third chance fission. This separation, shown in Fig. 12, is somewhat arbitrary because of inadequate information.

The ENDF/B-V evaluation of the  $^{235}\text{U}$  fission cross section was used to convert the evaluated ratios to  $^{240}\text{Pu}$  fission cross sections. If there are appreciable changes in the  $^{235}\text{U}$  fission cross-section standard for ENDF/B-VI, some revision of the present evaluation of  $^{240}\text{Pu}$  may be necessary. Figure 13 gives an overview of the  $^{240}\text{Pu}$  fission cross-section evaluation and a comparison with ENDF/B-V.

The total cross section below 300 keV is from the FITACS<sup>21</sup> fit described previously; above 300 keV the model calculations by Lagrange and Jary<sup>27</sup> were used. Figure 14 is a comparison of these results with ENDF/B-V and the measurements of Poenitz *et al.*<sup>17</sup> and Gwin *et al.*<sup>16</sup>

The scattering cross sections and angular distributions were evaluated by Ed Arthur. His evaluation was based primarily on the coupled-channel

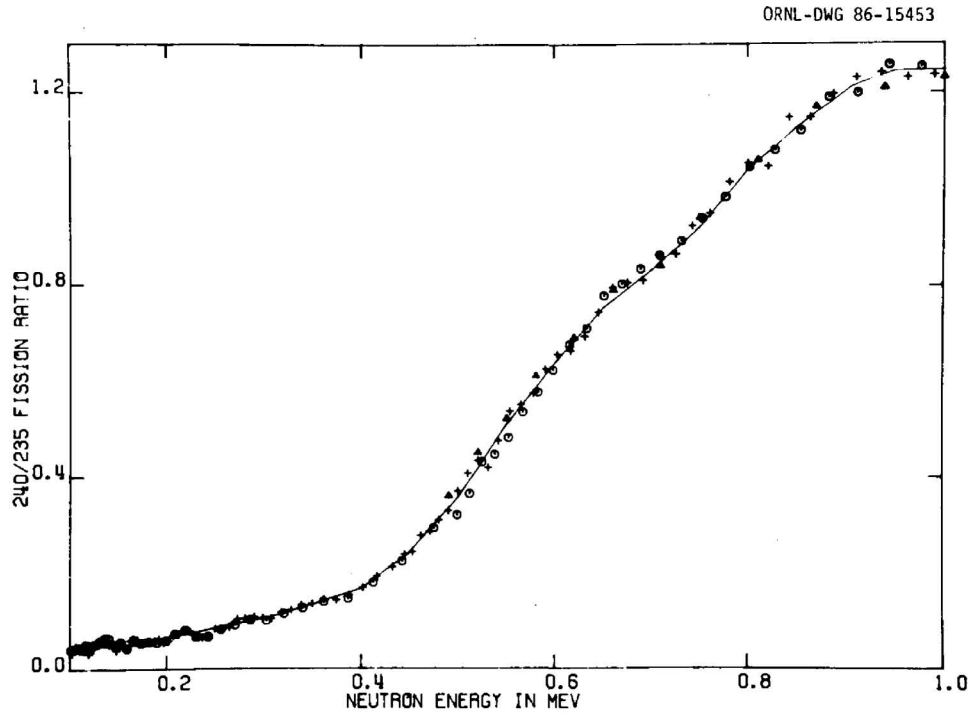


Figure 7. The fission cross section ratio to  $^{235}\text{U}$  from 100 to 1000 keV. The present evaluation (line) is unchanged from Version V. The circles are the measurements of Weston and Todd,<sup>29</sup> the triangles the data of Cierjacks *et al.*,<sup>30</sup> and the pluses are the data of Behrens *et al.*<sup>28</sup>

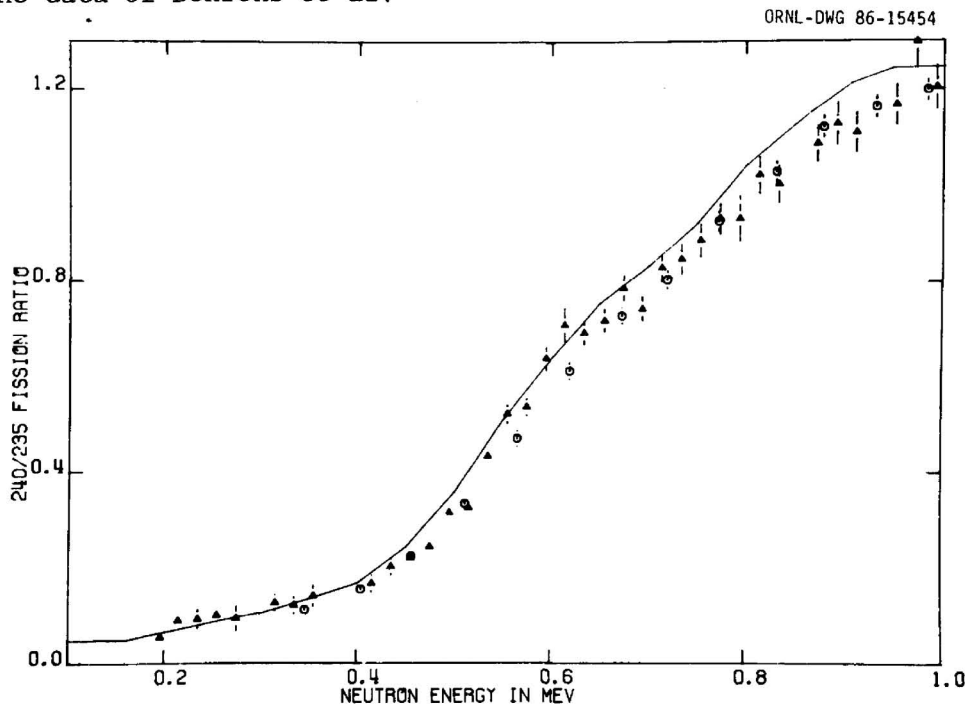


Figure 8. Comparison of the fission cross section ratio to  $^{235}\text{U}$  of ENDF/B-V (solid line) and the data of Meadows<sup>31</sup> (circles) and Butdz-Jørgensen and Knitter<sup>23</sup> (triangles).

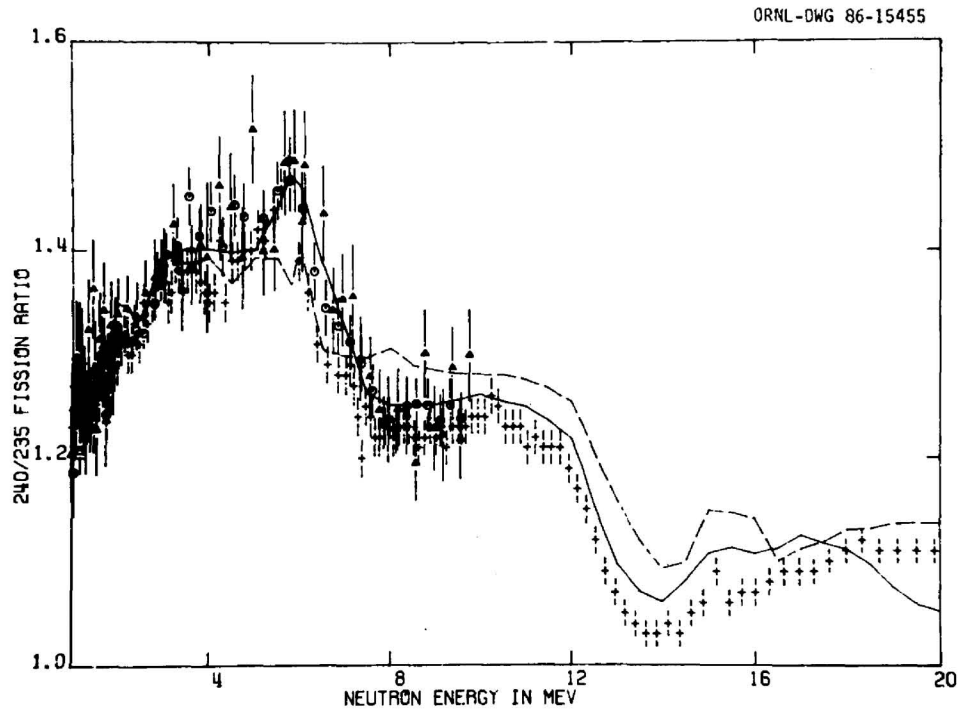


Figure 9. The fission cross section ratio to  $^{235}\text{U}$  from 1 to 20 MeV. The solid line is the present evaluation and the dashed line is ENDF/B-V. The circles are the data of Meadows;<sup>31</sup> the triangles are the data of Buttz-Jørgensen and Knitter;<sup>23</sup> the pluses are the data of Kari and Cierjacks.<sup>32</sup>

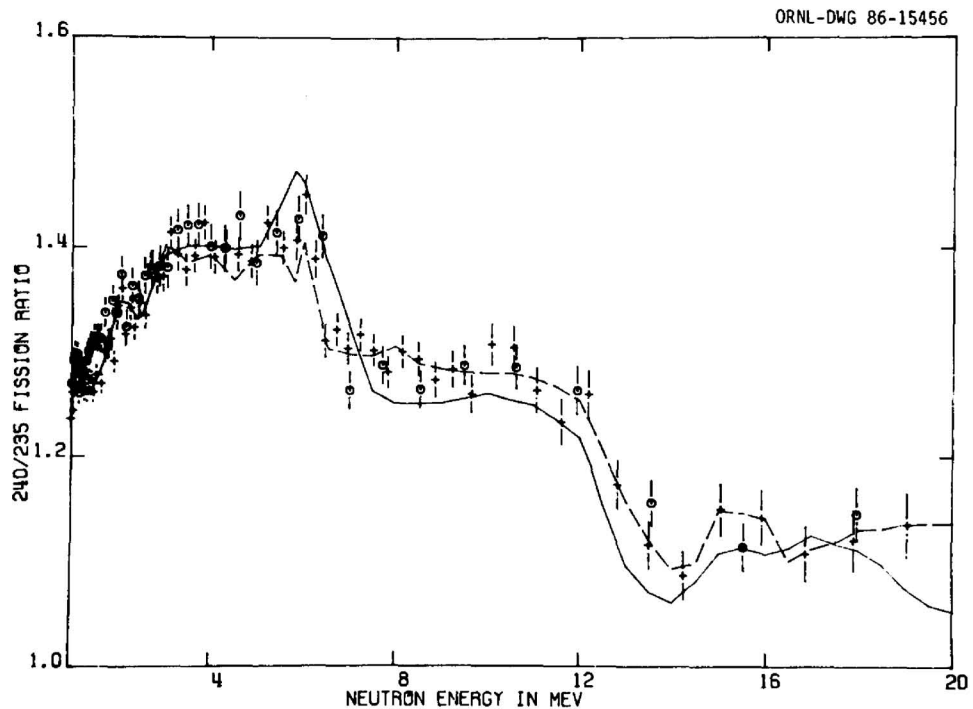


Figure 10. The fission cross section ratio to  $^{235}\text{U}$  from 1 to 20 MeV. The solid line is the present evaluation and the dashed line is ENDF/B-V. The circles are the data of Weston and Todd<sup>29</sup> and the pluses are the data of Behrens *et al.*<sup>28</sup>

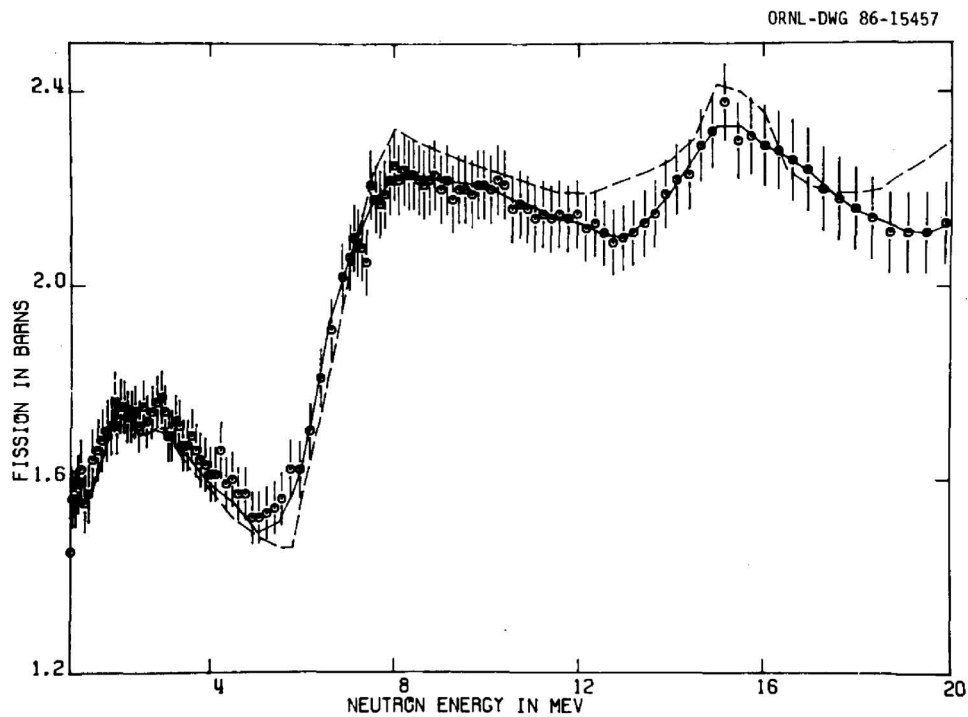


Figure 11. The fission cross section of  $^{240}\text{Pu}$  from 1 to 20 MeV. The solid line is the present evaluation and the dashed line is ENDF/B-V. The circles are the data of Kari and Cierjacks.<sup>32</sup>

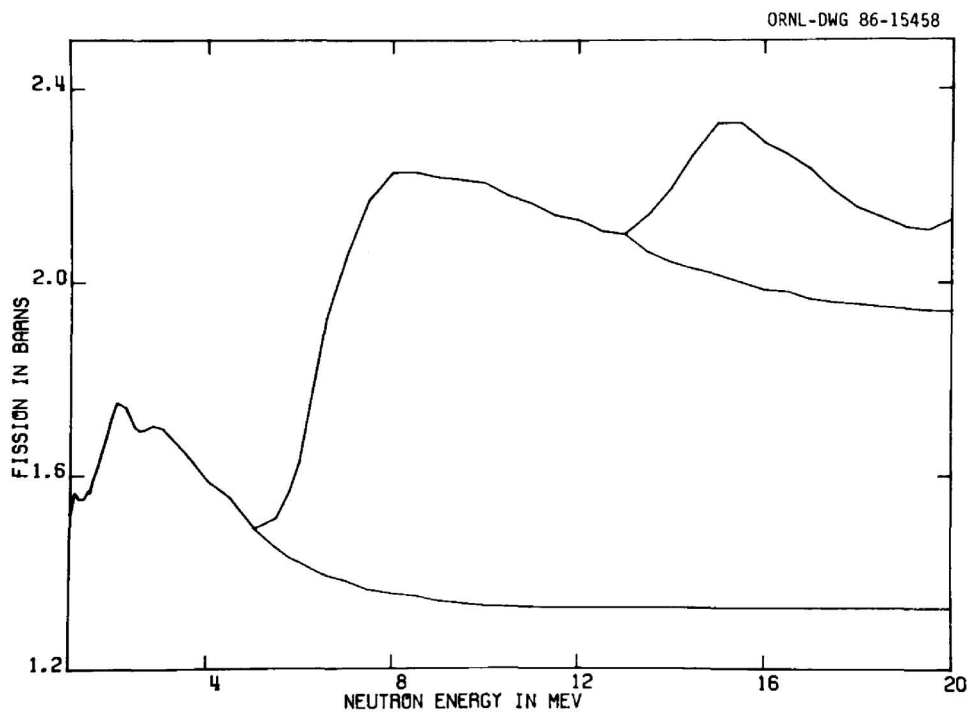


Figure 12. The evaluation of the fission cross section of  $^{240}\text{Pu}$  from 1 to 20 MeV and the separation into first, second and third chance fission. Note the displaced zero of the plot.

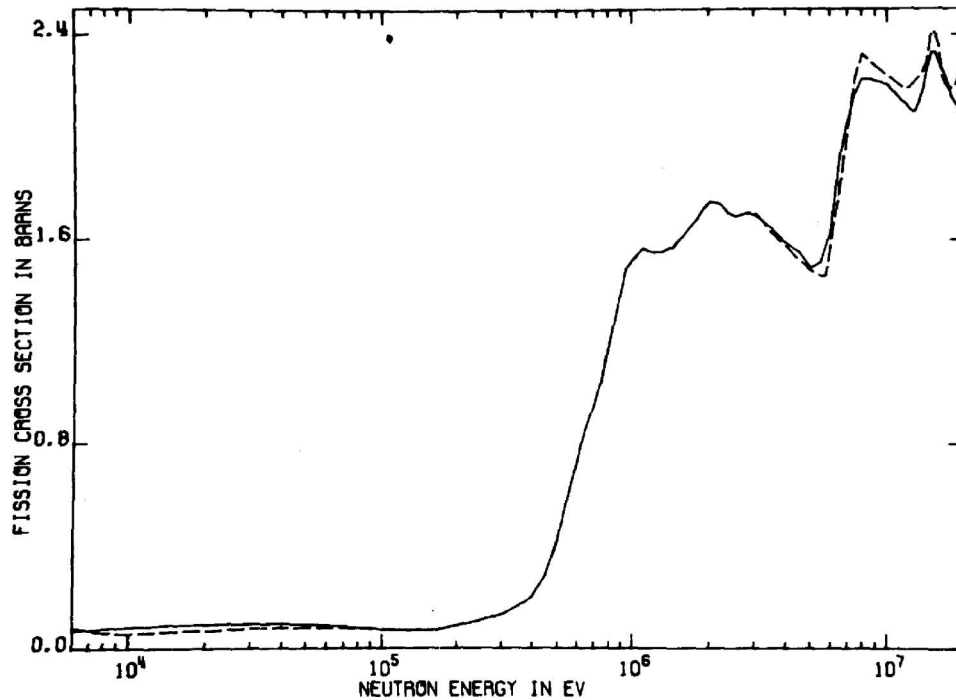


Figure 13. The evaluation of the fission cross section of  $^{240}\text{Pu}$  from 40 keV to 20 MeV as compared to ENDF/B-V (dashed line).

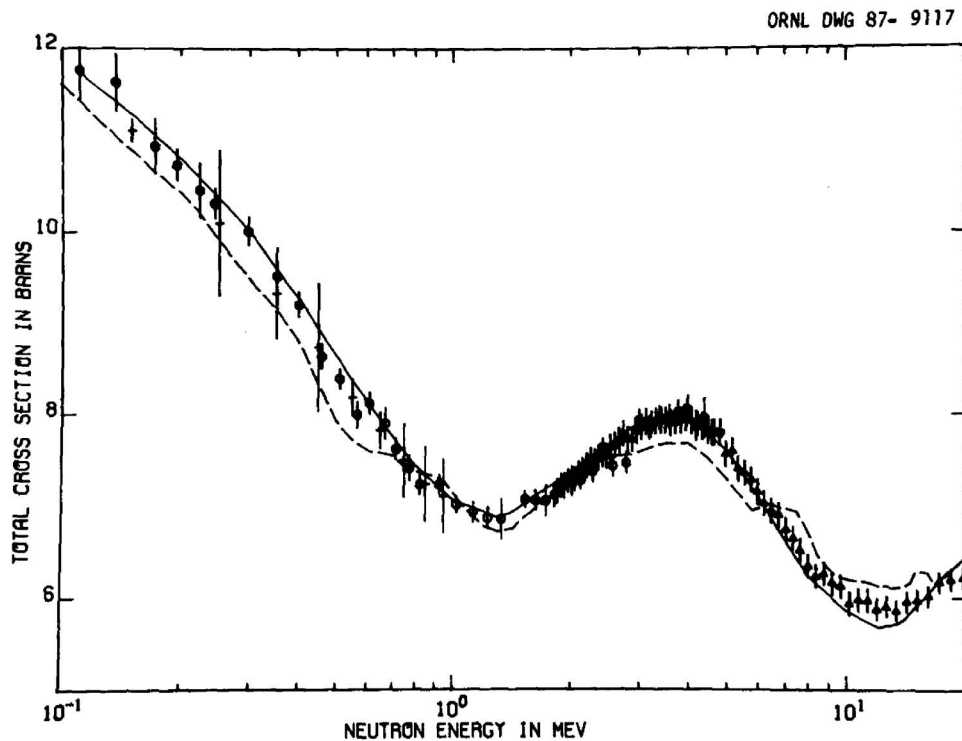


Figure 14. The evaluation (solid line) of the total cross section from 0.1 to 20 MeV. The dashed line is ENDF/B-V. The pluses are the data of Gwin<sup>16</sup> and the circles and triangles are the data of Poenitz *et al.*<sup>17</sup> Below 300 keV the evaluation was based on the FITACS<sup>21</sup> fit and at higher neutron energies the model calculations of Lagrange and Jary<sup>27</sup> were used.

calculations described by Lagrange and Jary<sup>27</sup> up to 3 MeV and on the Madland and Young<sup>33</sup> evaluation of  $^{242}\text{Pu}$  above 3 MeV. Several changes were incorporated in order to obtain smooth transition regions and agreement with the total cross sections. The first two levels and the total inelastic scattering are compared with ENDF/B-V in Fig. 15. The total inelastic and continuum inelastic are shown in Fig. 16 along with ENDF/B-V. Figure 17 shows all inelastic scattering cross sections for the present evaluation.

A comparison with the inelastic scattering measurements of Smith *et al.*<sup>34</sup> is shown in Fig. 18. None of the data points contained the contribution from the first inelastic level so this contribution has been subtracted from the evaluation. The two higher energy points included no contribution from the 142-keV level so this contribution has been subtracted from the solid line comparison, and the agreement with these two data points is excellent. The three lower energy points were quoted as containing the contribution from the 142-keV level so the solid line is a comparison with the present evaluation. The agreement is within the uncertainties of the evaluation and measurements. Because of the experimental neutron-energy resolution and the proximity of the 142-keV contribution to the elastic scattering, there is probably some contribution from this level lost from the lower three points.<sup>35</sup> The upper limit for this effect is indicated by the dashed line.

The model calculations of Lagrange and Jary<sup>27</sup> were also used for the total (n,2n) and (n,3n) cross sections. Comparisons with ENDF/B-IV and ENDF/B-V are shown in Fig. 19. Previous evaluations<sup>36</sup> were based on  $^{239}\text{Pu}$  data due to lack of experimental data.

The elastic scattering cross section was adjusted in order to maintain consistency between the total and partial cross sections. As can be seen in Fig. 20, where the total and elastic scattering cross sections are plotted, the shape of the elastic scattering cross section appears reasonable.

Uncertainties for the unresolved resonance region and the smooth cross sections (file 3) were evaluated for Revision 2 of ENDF/B-V and are unchanged for this evaluation.

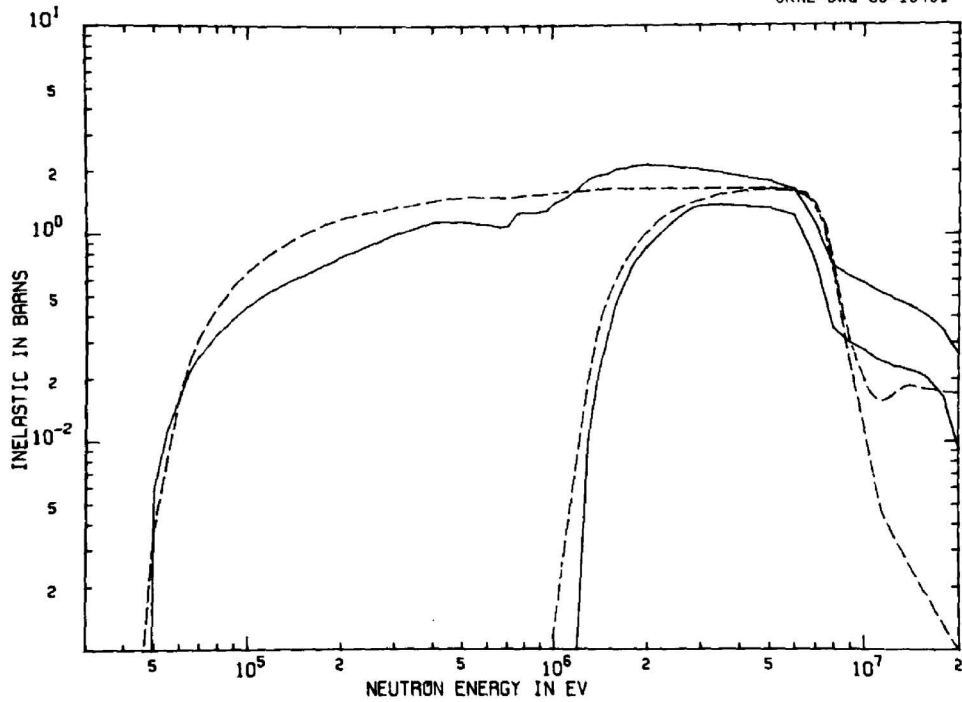


Figure 15. The evaluation (solid line) of the total inelastic scattering and the inelastic scattering from the first two levels for  $^{240}\text{Pu}$ . The dashed lines are the corresponding ENDF/B-V evaluations.

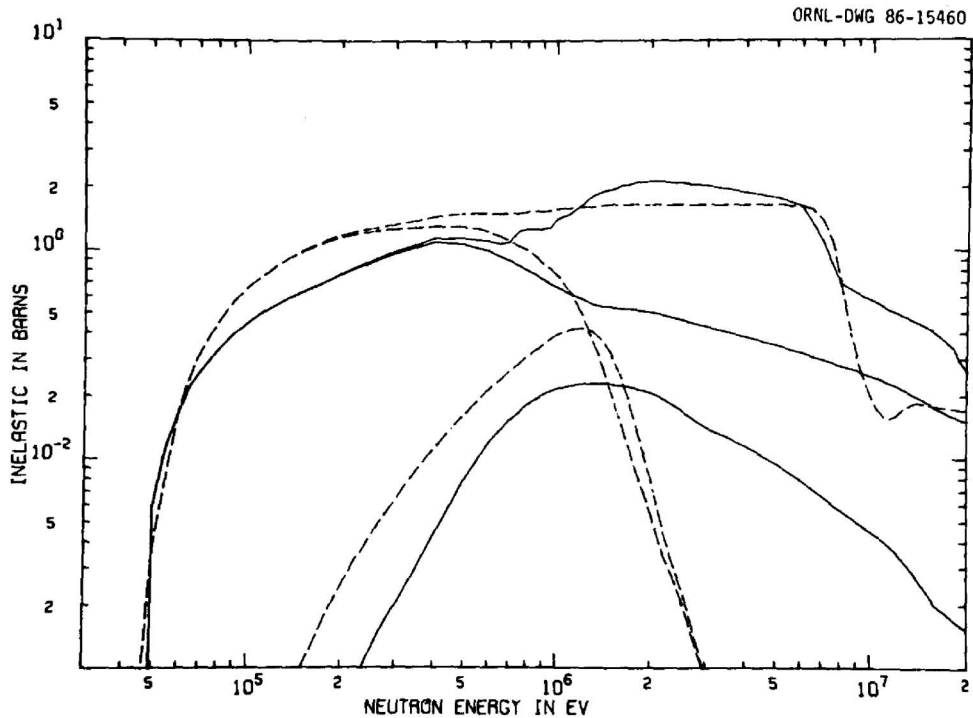


Figure 16. The evaluation (solid line) of the total inelastic scattering and the continuum contribution for  $^{240}\text{Pu}$ . The dashed lines are the corresponding ENDF/B-V evaluations.

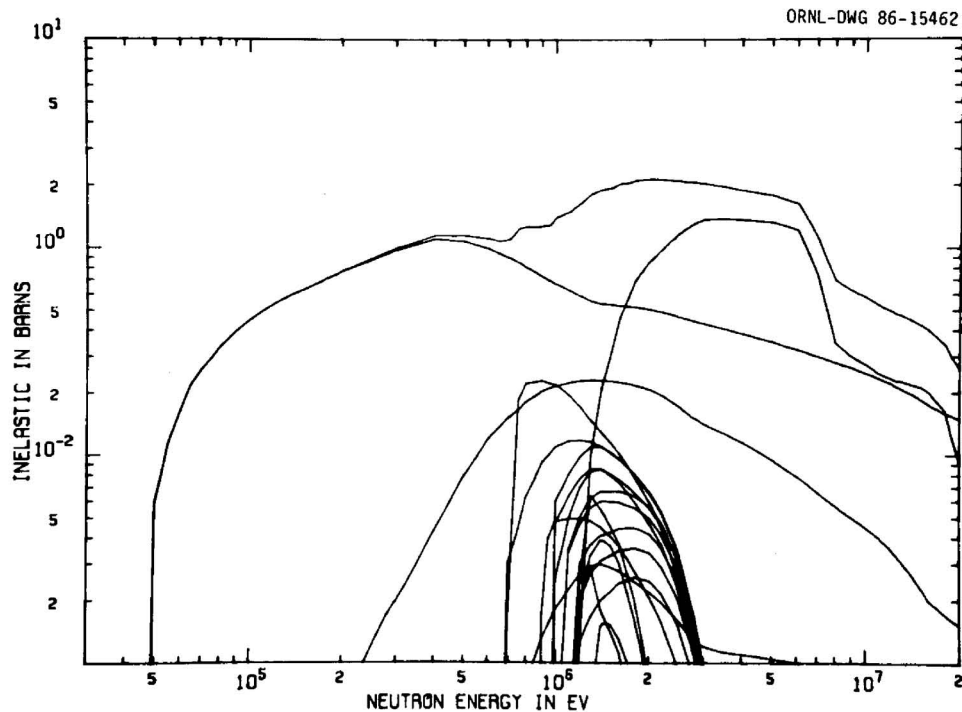


Figure 17. The evaluation of the total inelastic scattering and that of the individual levels for  $^{240}\text{Pu}$ .

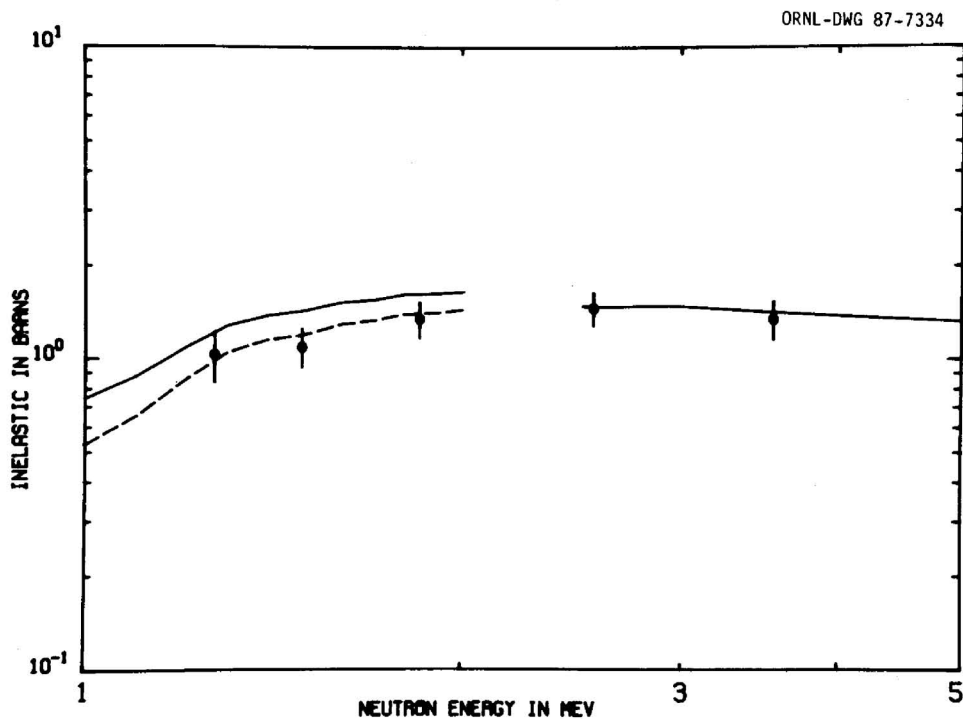


Figure 18. Comparison of the measurements of Smith, Guenther, and McKnight<sup>34</sup> with the present evaluation of inelastic scattering. None of the data points contain the first inelastic level and the two higher energy measurements do not contain the second level. The dashed line would be the case if the first three measurements also missed the second inelastic level.

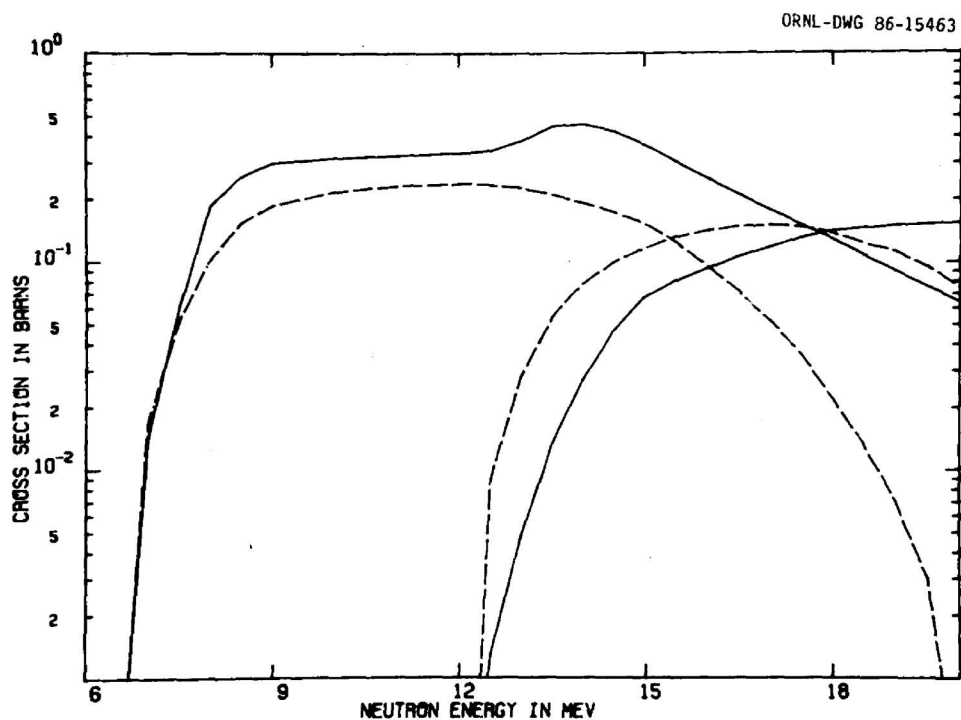


Figure 19. The accepted evaluation (solid line) by Lagrange and Jary<sup>27</sup> of the (n,2n) and (n,3n) cross sections for  $^{240}\text{Pu}$ . The dashed line is the corresponding ENDF/B-V evaluation.

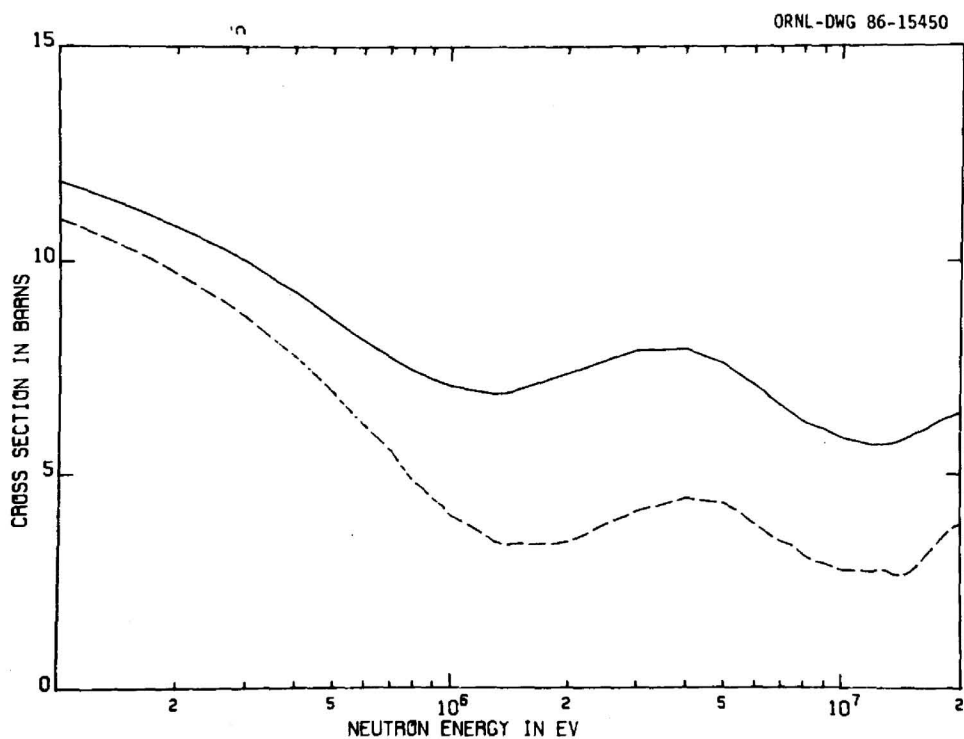


Figure 20. The evaluation of the total and elastic scattering (dashed line) cross sections from 0.1 to 20 MeV.

## 5. ANGULAR AND ENERGY DISTRIBUTIONS OF NEUTRONS

### 5.1 ELASTIC SCATTERING

The angular dependences for the elastically scattered neutrons were taken from the evaluation of  $^{242}\text{Pu}$  by P. G. Young and D. G. Madland of Los Alamos. This evaluation is described in some detail in Ref. 33. Because  $^{240}\text{Pu}$  and  $^{242}\text{Pu}$  have the same ground-state rotational band, they should be quite similar. The  $^{242}\text{Pu}$  evaluation was based on coupled channel calculations to which an isotropic compound nucleus contribution was added to the shape elastic scattering.

### 5.2 INELASTIC SCATTERING

The inelastic scattering angular distributions were taken from the Young and Madland evaluation of  $^{242}\text{Pu}$  (Ref. 33). The first three levels of  $^{240}\text{Pu}$  and  $^{242}\text{Pu}$  have the same spin and parity and the distributions are anisotropic. All other inelastic neutrons were assumed to be emitted isotropically. A preequilibrium component was ignored in this evaluation.

### 5.3 NEUTRON ENERGY DISTRIBUTIONS

The (n,2n), (n,3n), and fission neutron energy distributions were not changed from Version V. The inelastic scattering distributions are different because MF = 4 was changed, the exception being for MT = 91.

## 6. OTHER FILES

Many of the ENDF/B-V files were left intact for Version VI. For example, no changes were made in prompt or delayed  $\bar{\nu}$ , fission product yield data, radioactive decay data, the uncertainty files (which were modified in Revision 2) except for the 1.056-eV resonance, or the gamma-ray production files.<sup>37</sup> The latter date back to Version IV, but, since multiplicities were used below about 1 MeV, the newly revised capture and fission cross sections will produce different gamma-production cross sections at low energies.

## 7. CONCLUSIONS

This evaluation has taken into account many new measurements and model code results that were not available for ENDF/B-V. In particular, measurements have recently been made of: the parameters of the 1.056-eV resonance,<sup>7,8</sup> fission widths for subthreshold fission resonances,<sup>13</sup> fission cross sections,<sup>24,25,29,31,32</sup> and total cross sections.<sup>16-18</sup> Below 100 keV, the code FITACS by F. H. Fröhner<sup>21</sup> was used in addition to URES by E. Pennington.<sup>26</sup> In the MeV range, the Lagrange and Jary calculations<sup>27</sup> of the total, (n,2n), and (n,3n) were incorporated and the coupled-channel calculations for <sup>242</sup>Pu by Madland and Young<sup>33</sup> were used for the elastic and inelastic angular distributions. In addition, Ed Arthur relied heavily on the Lagrange and Jary results<sup>27</sup> for his treatment of the inelastic cross sections.

The data base for <sup>240</sup>Pu appears fairly good with a few exceptions; the parameters of the 1.056-eV resonance are not known with sufficient precision and the capture cross section in the keV and higher neutron energy region may not be accurate enough for some breeder reactor applications. Except for fission cross-section measurements, there is a paucity of experimental data above 100 keV. The new measurements of subthreshold fission and the ratio of <sup>240</sup>Pu to <sup>235</sup>U fission should give the fission cross sections to sufficient accuracy for most applications. If neutron emission above about 10 MeV is important, pre-equilibrium neutrons need to be included in the model calculations.

Figure 21 gives an overview of the cross sections in the present evaluation of <sup>240</sup>Pu.

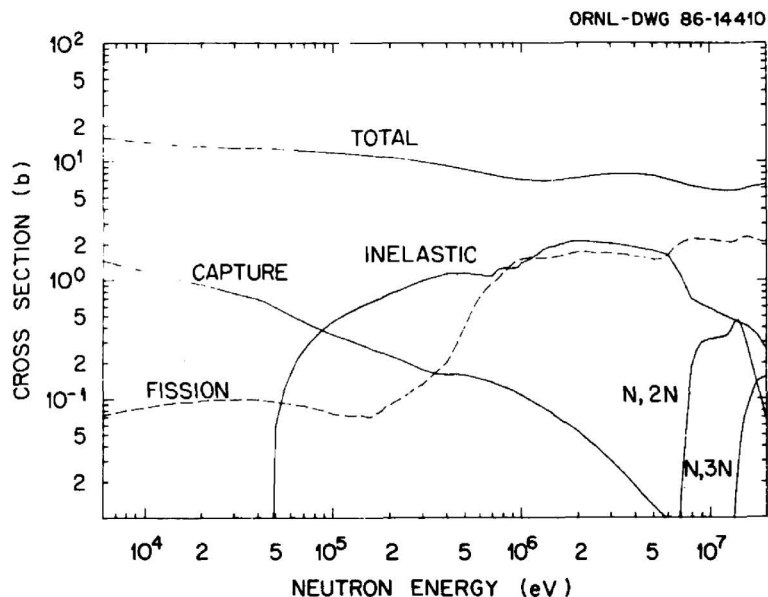


Figure 21. Overview of the present evaluation of  $^{240}\text{Pu}$  above the resolved resonance region.

#### ACKNOWLEDGEMENTS

The help, guidance, and editing of L. Stewart of LANL is gratefully acknowledged. R. Q. Wright of ORNL modified his code NPTXS and made it available to the author. F. H. Fröhner of KFK was very helpful in making his code FITACS available. R. R. Spencer provided many helpful discussions concerning the 1-eV resonance.

## REFERENCES

1. ENDF/B-V data file for  $^{240}\text{Pu}$  (MAT 1380), evaluated by L. W. Weston *et al.* of the Cross Section Evaluation Working Group, BNL-NCS-17541 (ENDF-201), 3rd Ed. (ENDF/B-V), R. Kinsey Editor, available from the National Nuclear Data Center, Brookhaven National Laboratory (July 1979).
2. L. W. Weston and R. Q. Wright, "Evaluation of the Fission and Capture Cross Sections of  $^{240}\text{Pu}$  and  $^{241}\text{Pu}$  for ENDF/B-V," p. 464 in *Proc. Int. Conf. Nuclear Cross Sections for Technology*, Knoxville, TN, Oct. 22-26, 1979, NBS SP 594 (1980).
3. ENDF-201 SUPPLEMENT 1, ENDF/B-V.2 SUMMARY DOCUMENTATION, p.191, BNL-NCS-17541, 3rd ed.(ENDF/B-V)SUPPLEMENT 1, B. A. Magurno and P. G. Young Editor, available from the National Nuclear Data Center, Brookhaven National Laboratory (Jan. 1985).
4. Odelli Ozer, "Nuclear Data Needs for LWR Applications," p. 464 in *Proc. Int. Conf. Nuclear Cross Sections for Technology*, Knoxville, TN, Oct. 22-26, 1979, NBS SP 594 (1980).
5. L. W. Weston, "Review of Microscopic Neutron Cross Section Data for the Higher Plutonium Isotopes in the Resonance Region," p. 1 in *Proc. Specialists' Mtg. on Nuclear Data of Pu and Am Isotopes for Reactor Applications*, Brookhaven National Laboratory, Nov. 20-21, 1978, BNL 50991, (1979).
6. M. Lounsbury, R. W. Durham, and G. C. Hanna, p. 287 in *Proc. Second Int. Conf. on Nuclear Data for Reactors*, Helsinki, IAEA, Vienna (1970).
7. H. I. Liou and R. E. Chrien, "Neutron Cross Sections and Doppler Effect of the 1.056 eV Resonance in  $^{240}\text{Pu}$ ," Brookhaven National Laboratory, private communication (1985).

8. R. R. Spencer et al., "Neutron Total Cross Section of  $^{240}\text{Pu}$  Below 6 eV and the Parameters of the 1.056 eV Resonance," p. 581 in *Proc. Int. Conf. Nuclear Data for Basic and Applied Science*, Santa Fe, NM, May 13-17 1985; also *Nucl. Sci. Eng.*, in press (1987).
9. H. Weigmann, G. Rohr, and F. Poortmans, "An Evaluation of  $^{240}\text{Pu}$  Resonance Parameters," p. 219 in *Proc. Conf. Resonance Parameters of Fertile Nuclei and  $^{239}\text{Pu}$* , Saclay, NEANDC(E) 163 U, Commissariat a l'Energie Atomique, Saclay (1974).
10. M. Ashgar, M. C. Moxon, and N. J. Pattenden, *Proc. Conf. Nuclear Data, Paris, 2*, 45, International Atomic Energy Agency, Vienna (1966).
11. R. W. Hockenbury, W. R. Moyer, and R. C. Block, *Nucl. Sci. Eng.* **49**, 153 (1972).
12. W. Kolar and K. H. Böckhoff, *Nucl. Energy* **22**, 299 (1968).
13. L. W. Weston and J. H. Todd, *Nucl. Sci. Eng.* **88**, 567 (1984).
14. G. F. Auchampaugh and L. W. Weston, *Phys. Rev.* **C12**, 1850 (1975).
15. E. Migneco and J. P. Theobald, *Nucl. Phys.* **A112**, 603 (1968).
16. R. Gwin, Oak Ridge National Laboratory, private communication (1985).
17. W. P. Poenitz, J. F. Whalen, and A. B. Smith, *Nucl. Sci. Eng.* **78**, 333 (1981); see also W. P. Poenitz and J. F. Whalen, "Neutron Total Cross Section Measurements in the Energy Region from 47 keV to 20 MeV," ANL/NDM-80, Argonne National Laboratory (1985); also private communication (1987).
18. F. Käppeler, Ly Di Hong, and H. Beer, "Neutron Total Cross Sections of  $^{240}\text{Pu}$  and  $^{242}\text{Pu}$  in the Energy Range from 10 to 375 keV," p. 49 in *Proc. of Specialists' Mtg. on Nuclear Data of Pu and Am Isotopes for Reactor Applications*, Brookhaven National Laboratory, Nov. 20-21, 1978, BNL 50991 (1979).

19. L. W. Weston and J. H. Todd, *Nucl. Sci. Eng.* **63**, 143 (1977).
20. K. Wisshak and F. Käppeler, *Nucl. Sci. Eng.* **66**, 363 (1978).
21. F. H. Fröhner, Kernforschungszentrum Karlsruhe, private communication (1982).
22. S. F. Mughabghab, *Neutron Cross Sections, Vol. 1, Neutron Resonance Parameters and Thermal Cross Sections*, p. 94-12, Academic Press, Orlando, Fla. 32887 (1984).
23. C. Budtz-Jørgensen and H. H. Knitter, *Nucl. Sci. Eng.* **79**, 380 (1981).
24. J. W. Behrens, *Nucl. Sci. Eng.* **85**, 314 (1983).
25. K. Wisshak and F. Käppeler, "Measurement of the Subthreshold Fission Cross Section of  $^{240}\text{Pu}$  and  $^{241}\text{Am}$ ," p. 893 in *Proc. Int. Conf. Neutron Physics and Nuclear Data*, Sept. 25-29, Harwell, England, PUBLICATIONS DE L'OCDE, Paris (1978).
26. E. Pennington (Argonne National Laboratory), Unresolved Resonance Program (UR), available from National Nuclear Data Center, Brookhaven National Laboratory (1973).
27. Ch. Lagrange and J. Jary, "Coherent Optical and Statistical Model Calculations of Neutron Cross Sections for  $^{240}\text{Pu}$  and  $^{242}\text{Pu}$  between 10 keV and 20 MeV," NEANDC (E) 198 "L", Commissariat a L'Energie Atomique, France (1978).
28. J. W. Behrens, J. C. Browne, and G. W. Carlson, "Measurement of the Neutron-Induced Fission Cross Sections of  $^{240}\text{Pu}$  and  $^{242}\text{Pu}$  Relative to  $^{235}\text{U}$ ," UCID-17047, Lawrence Livermore National Laboratory (1976); see also J. W. Behrens, R. S. Newbury, and J. W. Magana, *Nucl. Sci. Eng.* **66**, 433 (1978); see also J. W. Behrens, *Nucl. Sci. Eng.* **85**, 314 (1983).

29. L. W. Weston and J. H. Todd, *Nucl. Sci. Eng.* **84**, 248 (1983).
30. S. Cierjacks et al., p. 94 in *Proc. Specialists' Mtg. Fast Neutron Fission Cross Sections of  $^{233}$ ,  $^{235}$ , and  $^{239}\text{Pu}$* , Argonne, Illinois June 28-30, 1976, ANL-76-90, Argonne National Laboratory (1976).
31. J. W. Meadows, *Nucl. Sci. Eng.* **79**, 233 (1981).
32. K. Kari and S. Cierjacks, p. 57 in *Proc. Specialists' Mtg. Nuclear Data of Plutonium and Americium Isotopes for Reactor Applications*, Upton, New York, November 20-21, 1979, BNL-50991, Brookhaven National Laboratory (1979).
33. D. G. Madland and P. G. Young, "Evaluation of  $n + ^{242}\text{Pu}$  Reactions from 10 keV to 20 MeV," p. 189 in *Proc. Specialists' Mtg. Nuclear Data of Plutonium and Americium Isotopes for Reactor Applications*, Upton, New York, November 20-21, 1979, BNL-50991, Brookhaven National Laboratory (1979).
34. A. B. Smith, P. T. Guenther, and R. D. McKnight, "On the Neutron Inelastic-Scattering Cross Sections of  $^{232}\text{Th}$ ,  $^{233}\text{U}$ ,  $^{235}\text{U}$ ,  $^{238}\text{U}$ ,  $^{239}\text{Pu}$ , and  $^{240}\text{Pu}$ ," p. 39 in *Proc. Conf. Nuclear Data for Science and Technology*, Antwerp, September 6-10, 1982, Central Bureau for Nuclear Measurements, Geel, Belgium (1987).
35. A. B. Smith, Argonne National Laboratory, private communication (1987).
36. R. W. Hunter, L. Stewart, and T. J. Hiron, "Evaluated Neutron-Induced Cross Sections for  $^{239}\text{Pu}$  and  $^{240}\text{Pu}$ ," LA-5172, p. 36, Los Alamos National Laboratory (1973).
37. R. E. Hunter and L. Stewart, "Evaluated Neutron-Induced Gamma-Ray Production Cross Sections for  $^{239}\text{Pu}$  and  $^{240}\text{Pu}$ ," LA-4901, Los Alamos National Laboratory (1972).

## INTERNAL DISTRIBUTION

- |                      |   |
|----------------------|---|
| 1. G. de Saussure    | 23. R. Q. Wright  |
| 2. J. K. Dickens     | 24. A. Zucker   |
| 3. C. Y. Fu          | 25. P. W. Dickson, Jr. (consultant)                           |
| 4. R. Gwin           | 26. Gene H. Golub (consultant)                                |
| 5. J. A. Harvey      | 27. R. M. Haralick (consultant)                               |
| 6. J. K. Ingersoll   | 28. D. Stiner (consultant)                                    |
| 7. R. L. Macklin     | 29-30. Central Research Library                               |
| 8. F. C. Maienschein | 31. Division Advisory Committee                               |
| 9. R. W. Peelle      | 32. ORNL Y-12 Technical Library<br>Document Reference Section |
| 10. R. B. Perez      | 33-37. Laboratory Records Department                          |
| 11. R. R. Spencer    | 38. Laboratory Records ORNL-RC                                |
| 12. J. H. Todd       | 39. ORNL Patent Office  |
| 13-22. L. W. Weston  |   |

## EXTERNAL DISTRIBUTION

40. Office of Assistant Manager for Energy Research and Development, Oak Ridge Operations Office, DOE, Oak Ridge, TN 37830
- 41-50. E. D. Arthur, Los Alamos National Laboratory, Los Alamos, New Mexico 87545
51. J. W. Behrens, National Bureau of Standards, Center for Radiation Research, Nuclear Radiation Division, Washington, D.C. 20234
52. R. C. Block, Department of Nuclear Engineering, Rensselaer Polytechnic Institute, Troy, New York 12181
53. R. E. Chrien, Physics Department, Bldg. 510A, National Nuclear Data Center, Brookhaven National Laboratory, Upton, New York 11973
54. F. H. Fröehner, Institut für Neutronenphysik und Reaktortechnik, Kernforschungszentrum Karlsruhe, Postfach 3640, 7500 Karlsruhe, Federal Republic of Germany
55. R. W. Hockenbury, Rensselaer Polytechnic Institute, Linear Accelerator Facility, Troy, New York 12181
56. R. E. Hunter, Los Alamos National Laboratory, P.O. Box 1663, Los Alamos, New Mexico 87545
57. F. Käppeler, Institut für Neutronenphysik und Reaktortechnik, Kernforschungszentrum Karlsruhe, Postfach 3640, 7500 Karlsruhe, Federal Republic of Germany
58. Y. Kikuchi, Nuclear Data, Division of Physics, Japan Atomic Energy Research Institute (JAERI), Tokai-Mura, Naka-Gun, Ibaraki-Ken 319-11, Japan
59. H. H. Knitter, Bureau Central de Mesures Nucleaires, Steenweg naar Retie, B-2440, Geel, Belgium
60. C. Lagrange, Service de Physique Neutronique et Nucleaire, Centre d'Etudes de Bruyeres-le-Chatel, B.P. n° 561, 92542, Montrouge, Cedex, France

61. D. G. Madland, Los Alamos National Laboratory, P.O. Box 1663, Los Alamos, New Mexico 87545
62. J. W. Meadows, Argonne National Laboratory, 9700 S. Cass Avenue, Argonne, Illinois 60439
63. E. Pennington, Argonne National Laboratory, 9700 S. Cass Avenue, Argonne, Illinois 60439
64. M. G. Sowerby, Nuclear Physics Division, Building 418, Atomic Energy Research Establishment, Harwell, Didcot, Oxon OX11 0RA, United Kingdom
65. L. S. Stewart, Los Alamos National Laboratory, P.O. Box 1663, Los Alamos, New Mexico 87545
66. S. L. Whetstone, Division of Nuclear Sciences, Office of Basic Energy Sciences, U.S. DOE, RM G-355, Washington, D.C. 20545
67. H. Weigmann, Bureau Central de Mesures Nucleaires, Steenweg naar Retie, B-2440, Geel, Belgium
68. K. Wisshak, Kernforschungszentrum Karlsruhe, Institut fur Kernphysik III, Postfach 3640, D-7500 Karlsruhe 1, Federal Republic of Germany
- 69-98. Technical Information Center
- 99-223. ENDF Distribution - National Nuclear Data Center, Bldg. 197D, Brookhaven National Laboratory, Upton, New York 11973



